

**OXYGEN ISOTOPE SYSTEMATICS OF CHONDRULES FROM THE PARIS CM2 CHONDRITE.** N. Chaumard<sup>1</sup>, C. Defouilloy<sup>1</sup>, N. T. Kita<sup>1</sup> and A. Hertwig<sup>1</sup>, <sup>1</sup>WiscSIMS, Department of Geoscience, University of Wisconsin-Madison, Madison, WI 53706, USA (chaumard@wisc.edu).

**Introduction:** CM chondrites are the largest group of carbonaceous chondrites (CCs). In addition, they were recognized as clasts in many other meteorite classes [e.g., 1, 2], hence their importance to deciphering the origin and evolution of the early Solar System. CMs experienced intense secondary processes and display a wide range of aqueous alteration features, i.e., from type 2.6 to 2.0 [e.g., 3–5]. Paris is the least-altered CM chondrite described so far [6], classified as type 2.7 [7]. However, Paris contains both highly and less altered lithologies, the latter being of type 2.9 [6] based on the PCP index of [4]. The bulk O-isotope ratios of the altered ( $\delta^{17}\text{O}=0.54\text{‰}$ ;  $\delta^{18}\text{O}=6.51\text{‰}$ ) and less altered ( $\delta^{17}\text{O}=-1.30\text{‰}$ ;  $\delta^{18}\text{O}=4.32\text{‰}$ ) lithologies of Paris define an oxygen isotope mixing line passing through the CM2 and CO3 falls domains with variation explained by local differences in the extent of the alteration [6, 8–9]. Previous SIMS O-isotope analyses of Murchison chondrules show that chondrules in CM2 and CO3 derived from common O-isotope reservoirs [10], while CM parent asteroid accreted a higher proportion of ice/water than CO [6]. To further investigate the nature of pristine chondrules from CM, we performed SIMS O-isotope measurements in chondrules from the less altered lithology of the Paris CM2 chondrite.

**Samples and Methods:** Based on chondrule Mg# (mol.% MgO/[MgO+FeO]) in coexisting olivine and pyroxene, we selected 28 chondrules consisting of 26 Type I (Mg# $\geq$ 90; 11 POP, 4 PO, 8 PP, 1 BO fragment, 1 GOP, 1 GP) and 2 Type II (Mg# $<$ 90; 3 PO) from the Paris CM chondrite for O-isotope analysis. We also analyzed two isolated olivine (Fo-rich) grains. Initial SEM-BSE-SEI and EDS analysis were obtained using a Hitachi S-3400 electron microscope, while quantitative analyses were performed on a CAMECA SX-Five FE. Oxygen 3-isotope ratios of olivine and pyroxene within chondrules were performed on the WiscSIMS CAMECA-IMS 1280 ion microprobe using multi-collector Faraday cups as described by [11]. To analyze as many grains as possible, even in chondrules containing only small grains ( $<$  ca. 15 $\mu\text{m}$ ), we used a Cs<sup>+</sup> primary beam tuned to produce a 15  $\mu\text{m}$  and 10  $\mu\text{m}$  diameter spot with a primary ion intensity of  $\sim$ 3 nA and  $\sim$ 1 nA, respectively. External reproducibilities (2SD) were determined by intermittent measurements of San Carlos olivine. External reproducibilities for the 15  $\mu\text{m}$ -spot session are 0.2‰, 0.3‰, and 0.3‰ for

$\delta^{18}\text{O}$ ,  $\delta^{17}\text{O}$ , and  $\Delta^{17}\text{O}$ , respectively. For the 10  $\mu\text{m}$ -spot session, external reproducibilities are 0.4‰, 0.5‰, and 0.5‰ for  $\delta^{18}\text{O}$ ,  $\delta^{17}\text{O}$ , and  $\Delta^{17}\text{O}$ , respectively. A total of 229 SIMS analyses were obtained, with 4 to 12 analyses per chondrule to investigate the internal homogeneity of O-isotopes.

**Results and Discussion:** Oxygen isotope ratios of olivine, low-Ca and high-Ca pyroxene from all data plot between the CCAM [12] and Y&R [13] lines, mostly very close to the PCM [14] line. Regardless of the phases measured, 26 chondrules and the two Fo-rich grains have multiple analyses with indistinguishable  $\Delta^{17}\text{O}$  values (3 to 11 spots per chondrule/isolated grain), which define their host value and represent O-isotope ratios during chondrule melting [e.g., 14]. One PP chondrule shows entirely heterogeneous  $\Delta^{17}\text{O}$  values. Another GO chondrule has homogeneous olivine  $\Delta^{17}\text{O}$  values ( $-0.2\pm 0.4\text{‰}$ ) that is distinctly different from that of a single pyroxene analyses ( $-8\text{‰}$ ). Host  $\Delta^{17}\text{O}$  values were not determined for these chondrules.

The distribution of the host chondrule O-isotope ratios is similar to those in other CCs [14–20], with values ranging from  $-7.9\text{‰}$  to  $2.8\text{‰}$  and  $-11.1\text{‰}$  to  $-0.6\text{‰}$  for  $\delta^{18}\text{O}$  and  $\delta^{17}\text{O}$  (Fig. 1), respectively. Type I chondrules are <sup>16</sup>O-rich relative to Type II chondrules (Fig. 1), as observed in Acfer 094 and Y82094 (ungr. CCs), CO, CR, and CV chondrites [14–20].

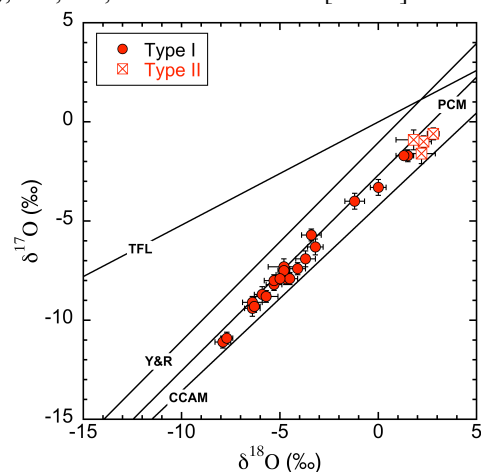


**Fig. 1:** Oxygen 3-isotope diagram of Paris chondrules. Each point represents the averaged, host value of a chondrule. Uncertainties are of 95% confident level.

Nine of 26 homogeneous chondrules have relict olivine and/or low-Ca pyroxene grains that deviate in  $\Delta^{17}\text{O}$  values more than the 3SD external reproducibil-

ity when compared to the host  $\Delta^{17}\text{O}$  value defined by the remaining analyses within the same single chondrule. This percentage of relict-grain bearing chondrules is similar to Murchison (CM2), Acfer 094, and CO chondrites [10, 14, 16]. However, the 22 relict grains found are either  $^{16}\text{O}$ -rich ( $n=9$ ) or  $^{16}\text{O}$ -poor ( $n=13$ ) compared to their host chondrules, defining a  $^{16}\text{O}$ -rich/ $^{16}\text{O}$ -poor ratio of relict grains ( $\sim 0.7$ ) slightly lower to that from Murchison, Acfer 094, and CO chondrites [10, 14, 16] ( $>0.9$ ). Nine relict grains have  $\Delta^{17}\text{O}$  values within the range of the host values calculated for other chondrules (from  $-7\%$  to  $-2\%$ ). The remaining are  $^{16}\text{O}$  enriched ( $\Delta^{17}\text{O}$ :  $-13\%$  and  $-9.5\%$ ) or  $^{16}\text{O}$  depleted ( $\Delta^{17}\text{O}$ : from  $-1.6\%$  to  $0.1\%$ ).

**Chondrule  $\Delta^{17}\text{O}$  vs. Mg#.** The averaged  $\Delta^{17}\text{O}$  values of individual chondrules from Paris range from  $-7\%$  to  $-3\%$  and from  $-3\%$  to  $-2\%$  for  $\text{Mg}\# >97$  and  $\text{Mg}\# <95$ , respectively (Fig. 2). This  $\text{Mg}\#$ - $\Delta^{17}\text{O}$  relationship is similar to those found in Murchison (CM2) [10], Acfer 094 [14], and the Y81020 CO3 chondrite [16], which confirms that chondrules formed in similar environments. However, Acfer 094 and Y81020 display a well defined bimodal distribution at  $-5.5\%$  and  $-2.5\%$ , while Paris and Murchison appear to display a continuum between  $-2\%$  and  $-3\%$  for  $\text{Mg}\#$ 's ranging from  $\sim 30$  to  $97$  (Fig. 2). In other words, the  $-2.5\%$  population of chondrules ( $\text{Mg}\#$ 's  $\sim 60$ – $70$ ) seems to not extend to highest  $\text{Mg}\#$ 's (up to  $\sim 97$ ) in CM chondrites.

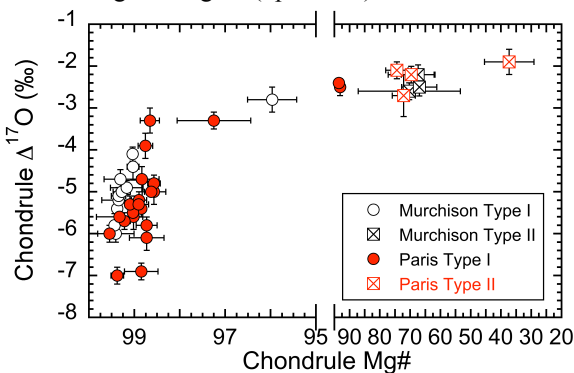


**Fig. 2:** Chondrule  $\text{Mg}\#$  vs. host  $\Delta^{17}\text{O}$  values.

As in the other groups of CCs [14–20], our data indicate that Paris sampled the  $\text{Mg}\# \sim 99$  reservoir ( $\Delta^{17}\text{O}$ :  $-5.5\%$ ). It supports the ubiquity of the  $^{16}\text{O}$ -rich chondrule-forming environment in the protoplanetary disk where CCs accreted. This reservoir existed under reducing conditions ( $f\text{O}_2 \sim -3.5$  log units below the IW buffer) and with a dust enrichment factors of  $100$ – $200$  [19]. The wide range of  $\Delta^{17}\text{O}$  values ( $-7\%$  to  $-3\%$ ) observed for chondrules with  $\text{Mg}\#$ 's  $\sim 99$  support an addition of a  $^{16}\text{O}$ -poor  $\text{H}_2\text{O}$  ice/water to the nearly anhydrous chondrule precursors to form more oxidized

chondrules with higher  $\Delta^{17}\text{O}$  values and lower  $\text{Mg}\#$ 's [19, 21]. In addition to a formation under more oxidizing conditions, the isotopic and chemical compositions of the  $^{16}\text{O}$ -poor chondrules in Paris ( $\Delta^{17}\text{O}$ :  $-2.7\%$  to  $-1.9\%$  for  $\text{Mg}\# \sim 75$ – $30\%$ ) may suggest higher and variable gas to dust ratios ( $\sim 300$ – $2000\times$ ; [19]) compared to  $^{16}\text{O}$ -rich chondrules.

**Implications for CM forming environments:** O 3-isotope analyses of Paris chondrules further suggest that similar chondrule populations were sampled by CM and CO chondrites across the snow line [10]. However, since CM chondrites do not show a clear bimodality in  $\Delta^{17}\text{O}$  as observed among chondrules in CO, they might accreted a slightly different population of chondrules compared to CO. According to Mn-Cr studies of secondary minerals, CM chondrites accreted later than CO ( $\sim 3.5$  Ma versus  $\sim 2.1$ – $2.4$  Ma after CAIs [22–23]). Therefore, it is possible that chondrule formation in CM accretion regions occurred much later than that of CO. Continuous  $\text{Mg}\#$ - $\Delta^{17}\text{O}$  relationship among CM chondrules may also suggest a single chondrule-forming environment that were increasingly enriched in water ice and dust with time. Assuming an accretion of the CO and CM parent bodies where their chondrules formed, our results can highlight the snow line moving towards the Sun and passing through the chondrule-forming region  $\sim 3$  Ma after CAIs [e.g., 24].

**References:** [1] Zolensky M. E. et al. (1996) *MAPS*, 31, 518–537. [2] Gounelle M. et al. (2003) *GCA*, 67, 507–527. [3] Zolensky M. E. et al. (1997) *GCA*, 61, 5099–5115. [4] Rubin A. E. et al. (2007) *GCA*, 71, 2361–2382. [5] Rubin A. E. (2015) *MAPS*, 50, 1595–1612. [6] Hewins R. H. et al. (2014) *GCA*, 124, 190–222. [7] Marrocchi Y. et al. (2014) *MAPS*, 49, 1232–1249. [8] Clayton R. N. & Mayeda T. K. (1999) *GCA*, 63:2089–2104. [9] Greenwood R. C. et al. (2014) *LPS XLV*, Abstract #2610. [10] Chaumard N. et al. (2016) *MAPS*, 51, A114–A692. [11] Kita N. T. et al. (2010) *GCA*, 74, 6610–6635. [12] Clayton R. N. et al. (1977) *EPSL*, 34, 209–224. [13] Young E. D. and Russell S. S. (1998) *Science*, 282, 1874–1877. [14] Ushikubo T. et al. (2012) *GCA*, 90, 242–264. [15] Rudraswami N. G. et al. (2011) *GCA*, 75, 7596–7611. [16] Tenner T. J. et al. (2013) *GCA*, 102, 226–245. [17] Schrader D. L. et al. (2013) *GCA*, 101, 302–327. [18] Schrader D. L. et al. (2014) *GCA*, 132, 50–74. [19] Tenner T. J. et al. (2015) *GCA*, 148, 228–250. [20] Tenner T. J. et al. (in press) *MAPS*. [21] Connolly, Jr. H. C. & Huss G. R. (2010) *GCA*, 74, 2473–2483. [22] Fujiya W. et al. (2012) *Nature Comm.*, 3, 627. [23] Doyle P. M. et al. (2015) *Nature Comm.*, 6, 7444. [24] Martin R. G. and Livio M. (2012) *MNRAS* 425, L6–L9.